Journal of Electroceramics, 7, 179–188, 2001

Electrode-Contact Spreading Resistance Phenomena in Doped-Lanthanum Gallate Ceramics

E.J. ABRAM, D.C. SINCLAIR & A.R. WEST
Department of Engineering Materials, University of Sheffield, Mappin Street, Sheffield, S1 3JD, UK

Submitted July 23, 2001; Revised July 23, 2001; Accepted October 29, 2001

Abstract. Impedance spectra of $La_{0.8}Sr_{0.2}Ga_{0.83}Mg_{0.17}O_{2.815}$ ceramics were measured using gold and platinum paste, and sputtered gold electrodes. Impedance complex plane plots, Z^*, for samples with sputtered gold electrodes consist of a single arc associated predominantly with the bulk response and a low frequency 'spike' associated with electrode-polarisation and diffusion-related phenomena. An additional arc at intermediate frequencies with an associated capacitance of the order of 1 nFcm^{-1} and a resistance with a similar temperature dependence to that of the bulk resistance is present in Z^* plots for samples measured using gold paste electrodes hardened at temperatures between 500 and 850°C. Scanning electron microscopy and impedance spectroscopy show the additional response to be a 'spreading resistance' caused by the electrodes making well-separated discrete contacts with the ceramic due to partial sintering of gold particles in the paste. Z^* plots for samples measured using platinum paste electrodes hardened between 725 and 1000°C exhibit a much smaller additional response with similar behaviour to that observed with gold paste electrodes but also showed an apparent increase in sample resistance due to significant loss of contact between sample and electrode in some regions of the interface.

Keywords: impedance spectroscopy, electrodes, spreading resistance, oxide-ion conductors, doped-lanthanum gallate

Introduction

The electrical microstructure of electroceramics, such as oxide-ion conducting lanthanum gallate-based ceramics, can be analysed by impedance spectroscopy. This technique can separate the behaviour of electroactive components in ceramics such as the bulk (intragranular regions) and grain boundaries. A schematic diagram of a typical impedance spectrum for a ceramic oxide-ion conductor, displayed as a complex plane plot (Z^*) with linear, equally-scaled axes, and its equivalent electrical circuit are shown in Fig. 1. A high frequency arc associated with the bulk response and an intermediate frequency arc associated with a grain boundary response are usually present. At low frequencies, a response associated with electrode-polarisation and diffusion-related phenomena is normally observed. Such Z^* plots can be interpreted using the equivalent electrical circuit shown in Fig. 1, where R_b, R_{gb}, C_b, C_{gb} are the resistances and capacitances of the bulk and grain boundary components, respectively. Typical geometry-normalised capacitances for bulk and grain boundary components are of the order of 10^{-12} Fcm^{-1} and 10^{-11} to 10^{-8} Fcm^{-1}, respectively. In general the circuit element(s) representing the response of the electrode depends on the nature of the electrochemical reaction occurring at the sample-electrode interface but usually has a capacitive component(s) with a value(s) between 10^{-7} and 10^{-5} Fcm^{-1} [1].

The form of the electrode response in Z^* plots depends on many factors, including the electrode material, sample roughness, temperature and oxygen partial pressure at which measurements are performed, and the measured frequency range. Generally, in the case of electrodes that block oxygen diffusion, oxide-ions pile up at the ceramic-electrode interface and the electrode response can be modelled as an ideal capacitor. This leads to a vertical 'spike' in Z^* plots for completely blocking-electrodes. Electrodes that are partially-blocking allow limited diffusion and lead to

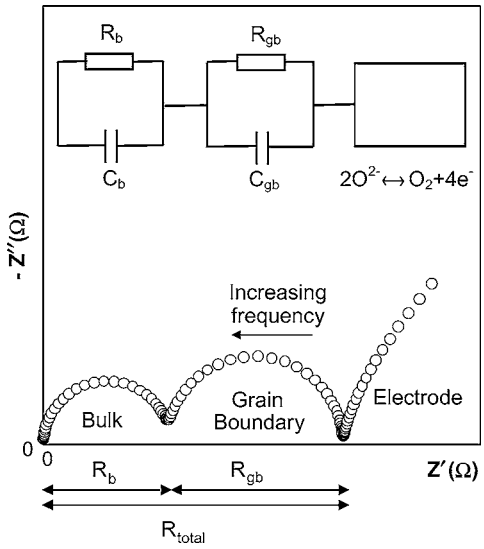

Fig. 1. Schematic diagram of a typical impedance spectrum, displayed as a complex plane plot (Z^*), of an oxide-ion conducting ceramic, and its equivalent electrical circuit.

an inclined spike. In cases where oxygen molecules are unable to diffuse through the entire thickness of the electrode at the lowest frequencies, the ideal electrode response is an inclined spike with a 45° angle to the vertical, a so-called Warburg-response. However at high temperatures and/or lower frequencies the spike may collapse to a semicircular arc, indicating oxygen molecules are able to diffuse through the entire thickness of the electrode at low frequencies. It is also possible to observe a semicircular 'charge-transfer' arc associated with electron transfer to and from the oxide-ions at the ceramic-electrode interface [1].

Low frequency impedance data can also be influenced by the quality of the contact at the ceramic-electrode interface. Hwang et al. [2] have shown that incomplete contact between gold foil electrodes and roughened cerium dioxide ceramic surfaces leads to an additional arc in Z^* plots with an associated capacitance of ~4 pF. This value was approximately four times higher than the bulk capacitance, and they showed that isolated metal electrode-ceramic contacts caused the additional arc in the Z^* plots due to 'spreading resistance'. The spreading resistance response was observed in addition to the electrode response(s) described above. Similar interfacial responses have also been observed for yttria-stabilised zirconia (YSZ)–$YBa_2Cu_3O_{7-x}$ interfaces [3], and YSZ films with gold paste electrodes [4].

Spreading resistances can be explained assuming idealised isolated circular contacts on the surface of a resistive sample. An isolated circular contact of radius a and infinite conductivity on the surface of a resistive sample, has an associated electrode-sample spreading resistance (R_{sp}) and capacitance (C_{sp}) given by:

$$R_{sp} = (4a\sigma)^{-1} \quad (1)$$

$$C_{sp} = 4a\varepsilon_r\varepsilon_0 \quad (2)$$

where ε_0 is the permittivity of free space, and σ and ε_r are the conductivity and relative permittivity of the sample, respectively [2, 5]. Application of a positive voltage to the contact causes the local electric field to diverge into the sample. This leads to a spreading resistance (R_{sp}) within the sample and an associated capacitance (C_{sp}) at the contact-sample interface. In the case of a planar electrode with multiple point contacts on a ceramic, each contact has an associated spreading resistance (R_{sp}) and capacitance (C_{sp}). Provided the inter-contact distance is large relative to the radii of the contacts then

$$R_{spt} = (4\Sigma a\sigma)^{-1} \quad (3)$$

$$C_{spt} = 4\Sigma a\varepsilon_r\varepsilon_0 \quad (4)$$

where R_{spt} and C_{spt} are the total spreading resistance and capacitance, and $\sum a$ is the sum of the radii of the individual contacts [2, 6]. The effect is illustrated schematically in Fig. 2 for an electrode making an array of isolated contacts with the surface of an oxide-ion conducting ceramic. A parallel element with a resistor, R_{spt}, representing the total spreading resistance, a capacitor, C_{spt}, representing the total capacitance of the electrode contacts, and another capacitor, $C_{\text{air gaps}}$, representing the total capacitance of the air gaps between the contacts, is connected in series with the circuit used to represent the electrical microstructure of the ceramic as shown in Fig. 3. The two capacitors in the additional circuit element can be summed to give a single parallel

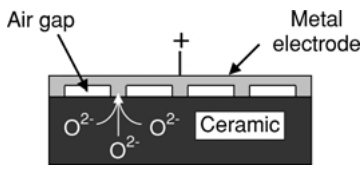

Fig. 2. Schematic diagram of oxide-ion motion in the vicinity of an electrode making an array of discrete contacts on the surface of an oxide-ion conducting ceramic.

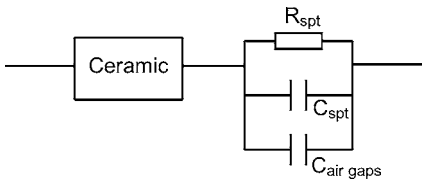

Fig. 3. Equivalent electrical circuit for spreading resistance phenomena on a ceramic. R_{spt} and C_{spt} represent the total spreading resistance and capacitance, respectively and $C_{air\ gaps}$ represents the capacitance of the air gaps between the contacts. The equivalent circuit for the ceramic is shown as a single-lumped element.

resistor-capacitor element. This additional circuit element leads to an additional arc in Z^* plots. The inclusion of $C_{air\ gaps}$ is necessary because according to Eq. (4), the capacitance associated with the additional response, C_{spt}, would be expected to be lower than that of the ceramic. This is not found experimentally, and it is the presence of air gaps between the electrode contacts that leads to an additional response with a higher capacitance than that of the ceramic [2].

In this study, impedance spectroscopy was performed on $La_{0.8}Sr_{0.2}Ga_{0.83}Mg_{0.17}O_{2.815}$ ceramics using gold and platinum paste, and sputtered gold electrodes. The effects of varying hardening temperatures for gold and platinum paste electrodes on the response in Z^* plots, and differences in the response in Z^* plots using the three types of electrodes, were investigated. The morphology of the electrodes was characterised by scanning electron microscopy (SEM), and these observations were correlated with the spreading resistance-type behaviour observed for the various electrode contacts.

Experimental

$La_{0.8}Sr_{0.2}Ga_{0.83}Mg_{0.17}O_{2.815}$ (LSGM) ceramics were synthesised by a solid state route. Stoichiometric amounts of La_2O_3 (99.99% pure), Ga_2O_3 (99.995%), MgO (reagent grade) and $SrCO_3$ (99.9%+) powders were milled in de-ionised water using zirconia-based media. The La_2O_3 and MgO powders were dried at 1000°C prior to weighing. The mixture was calcined at 1250°C for 6 hours, then milled again. Pellets were cold-pressed uniaxially at 50 MPa, and sintered at 1470°C for 6 hours. The phase purity of the ceramics was checked by X-ray diffraction (XRD) and scanning electron microscopy (SEM). Pellet densities were estimated using their masses and dimensions.

Impedance spectroscopy (IS) was performed in air on the LSGM ceramics at frequencies ranging from 5 Hz to 13 MHz between 25 and 450°C using a Hewlett Packard 4192A impedance analyser. Gold paste (Engelhard-CLAL, T10112), platinum paste (Engelhard-CLAL, 6082) and sputtered gold electrodes were used. The gold and platinum pastes were smeared onto the parallel faces of the ceramics, dried at 200°C then hardened at temperatures up to 1000°C in air. Sputtered gold electrodes were deposited for 8 minutes at 20 mA current under argon using an Emscope SC500 gold sputter-coater. All data were corrected for the geometric factor of the ceramics (thickness/electrode area). Capacitance data were corrected for the parallel capacitance of the empty jig (∼6 pF) in which the samples were supported.

The effect of the gold and platinum paste hardening temperature on the response in Z^* plots of the LSGM ceramics was investigated. Gold paste electrodes were applied to a LSGM ceramic and dried at 200°C for 2 hours. This was repeated on another LSGM ceramic using platinum paste. The impedance response of each was measured in air. Both ceramics with the original dried electrodes were heated together at 500°C for 2 hours, then subsequently at 500, 650, 725, 800, 850 and 1000°C overnight. The impedance response of each was measured after each heat treatment. The effect of atmosphere on the response in Z^* plots obtained using gold paste electrodes was measured by allowing samples to equilibrate for approximately one hour in flowing argon before measuring.

To determine if specific impedance responses were caused by the use of gold paste electrodes or more generally gold metal electrodes, the following experiment was performed. Three LSGM ceramics, one with gold paste electrodes dried at 200°C for 2 hours, another with sputtered gold electrodes, and a blank with no electrodes were heated overnight in air at 650°C. Afterwards, the impedance spectra of the pellets were measured. Gold paste electrodes dried at 200°C for 2 hours were applied to the blank for impedance measurement after the heat treatment. A similar experiment was also performed in which the pellets were heated in flowing nitrogen as opposed to air, measured, then heated in oxygen overnight and re-measured.

The morphology of gold paste electrodes dried at 200°C for 2 hours and hardened at 350, 650 and 1000°C, platinum paste electrodes dried at 200°C for 2 hours and hardened at 650 and 1000°C, and sputtered gold electrodes was studied by secondary electron

imaging using a JEOL JSM 6400 scanning electron microscope. The impedance response of each sample was measured prior to mounting for SEM. The samples were mounted in resin, polished to a 1 μm finish perpendicular to the electrode-ceramic interface and coated with carbon to prevent charging in the microscope.

Results and Discussion

The LSGM ceramics were found to be phase-pure by XRD but SEM showed the presence of two secondary phases. Qualitative energy dispersive X-ray spectroscopy (EDS) on one of the secondary phases indicated a significantly lower La/Ga ratio than in the primary phase. The areas of the other secondary phase were too small to analyse. $LaSrGaO_4$ and $LaSrGa_3O_7$ were shown to be present in the calcined powder by XRD, and so these were assumed to be the secondary phases in the sintered ceramics. The grain size of the LSGM phase was in the range 5 to 30 μm. Pellet densities were approximately 95% of the theoretical X-ray density.

A Z^* plot for a LSGM ceramic measured at 328°C in air using sputtered gold electrodes is shown in Fig. 4(a) and shows an arc at high frequencies and a low frequency spike. The high frequency arc has an associated capacitance of about 6 pFcm^{-1}. A capacitance value of this order of magnitude is typical of a bulk (intragranular) response. Detailed curve fitting analysis of this arc shows the presence of a minor overlapping grain boundary response [7] but for this study the high frequency arc will be referred to as the bulk arc. The associated resistance of the bulk arc, R_b, is ~16 kΩcm. The low frequency spike has an associated capacitance of the order of 2 μFcm^{-1}, which is typical for polarisation associated with an electrochemical reaction involving mobile oxide-ions at the electrodes. A Z^* plot of the same LSGM ceramic measured at 329°C using platinum paste electrodes dried at 200°C for 20 minutes then hardened at 1000°C for 30 minutes is shown in Fig. 4(b). The response is similar to that obtained using sputtered gold electrodes. It consists of a high frequency bulk arc (R_b ~17 kΩcm) and the beginning of a low frequency electrode spike with associated capacitances of ~6 pFcm^{-1} and 9 μFcm^{-1}, respectively. More of the electrode spike is present in spectra measured at higher temperatures. The Z^* plot also has a small additional arc at intermediate frequencies with an associated capacitance and resistance of ~1 nFcm^{-1} and 1 kΩcm, respectively. A Z^* plot of the same LSGM ceramic measured at 328°C using gold paste electrodes dried at 200°C for 20 minutes then hardened at 800°C for 30 minutes is shown in Fig. 4(c). The spectrum is similar to that obtained using platinum electrodes, except that the additional arc at intermediate frequencies has a significantly larger associated resistance. The high frequency bulk arc (R_b ~ 17 kΩcm)

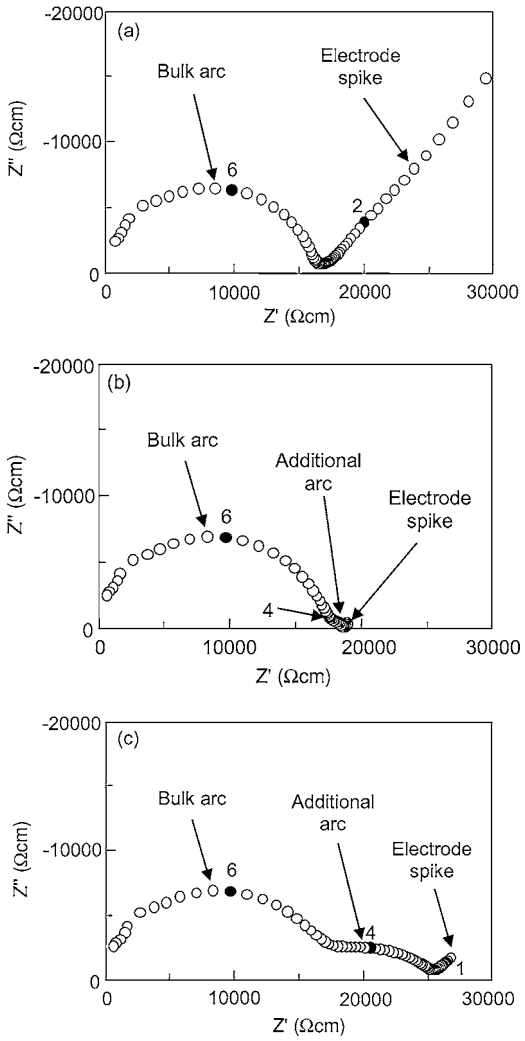

Fig. 4. Z^* plots for a LSGM ceramic measured at ~328°C using sputtered gold electrodes (a), platinum paste electrodes dried at 200°C for 20 minutes then hardened at 1000°C for 30 minutes (b), and gold paste electrodes dried at 200°C for 20 minutes then hardened at 800°C for 30 minutes in air (c). Selected frequencies (in Hz), on a logarithmic scale, are shown as filled circles.

and low frequency electrode spike have associated capacitances of $\sim$6 pFcm^{-1} and 17 μFcm^{-1}, respectively. The capacitance and resistance associated with the additional arc are $\sim$4 nFcm^{-1} and 7 kΩcm, respectively.

Associated capacitance values for this additional arc are typical of grain boundary responses, however, as Z^* plots of the same ceramic measured using sputtered gold electrodes do not show the additional arc, this eliminates the possibility that this arc is a grain boundary response. Clearly, it is caused by the use of gold paste electrodes, and to a limited extent, platinum paste electrodes.

Arrhenius plots of the bulk resistance, R_b, and the additional resistance, R_{add}, measured using gold and platinum pastes, and R_b for sputtered gold electrodes are shown in Fig. 5. R_b values are in good agreement for all three types of electrodes whereas R_{add} is almost two orders of magnitude greater for gold paste electrodes than for platinum paste electrodes. Activation energies for R_b and R_{add} are very similar, 1.1 and 1.0 ± 0.05 eV, respectively. The activation energy for electrical conduction in the ceramic is in agreement with the value of 1.076 ± 0.008 eV reported by Huang et al. [8].

Impedance spectra measured in air and argon of a LSGM ceramic using gold paste electrodes exhibiting the additional arc were very similar. Changing the atmosphere, therefore, had no significant effect on the associated resistance of the additional response, indicating that it was not due to a difference in dynamics of the charge transfer process occurring at the gold paste electrodes.

Z^* plots for a LSGM ceramic measured at 334°C using gold paste electrodes hardened at 200°C for 2 hours, then 650, 800 and 1000°C overnight are shown in Fig. 6. Heating at 200°C for 2 hours lead to Z^* plots dominated by a bulk arc and an electrode spike with a possible indistinct additional response at intermediate frequencies, Fig. 6(a). On heating at 650°C overnight an additional arc was present at intermediate frequencies with an associated resistance, R_{add}, approximately ten times higher than R_b, Fig. 6(b). Heating at subsequently higher temperatures caused R_{add} to decrease, Fig. 6(c)

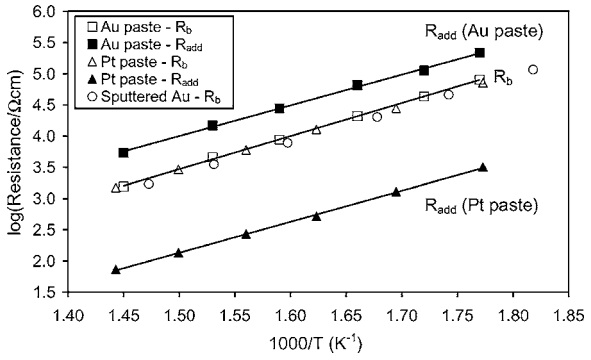

Fig. 5. Arrhenius plots of R_b and R_{add} for a LSGM ceramic with gold (Au) paste electrodes hardened at 650°C overnight, platinum (Pt) paste electrodes hardened at 1000°C for 30 minutes, and sputtered gold electrodes (no associated R_{add}).

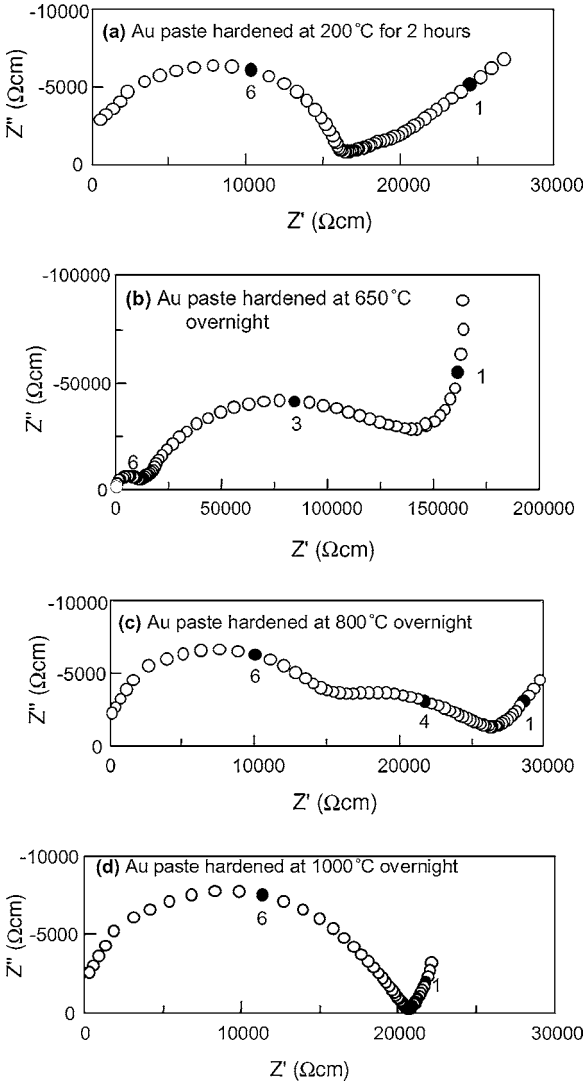

Fig. 6. Z^* plots of a LSGM ceramic measured at 334°C in air using gold paste electrodes hardened in air at 200°C for 2 hours (a), then 650 (b), 800 (c) and 1000°C (d) overnight. Selected frequencies (in Hz), on a logarithmic scale, are shown as filled circles. [Note: the difference in scale in (b) compared to (a), (c) and (d)].

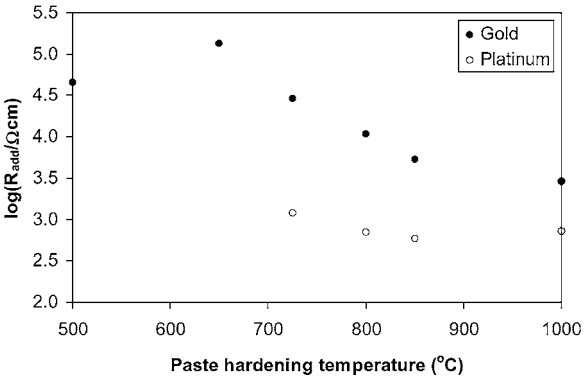

Fig. 7. R_{add} measured in air at 334°C as a function of gold and platinum paste electrode hardening temperature. The paste electrodes were dried onto LSGM ceramics at 200°C for 2 hours and heated at 500°C overnight, then subsequently at 650, 725, 800, 850 and 1000°C overnight in air.

and (d). After heating at 800°C overnight, R_{add} became approximately equal to R_b, and after heating at 1000°C overnight, the spectrum is dominated by the bulk arc and an electrode spike. This sample was post-annealed at 650°C overnight to determine if the large additional response could be re-introduced but the impedance spectrum was unchanged. The capacitance associated with the additional arc was ~1 nFcm^{-1}. After each heat treatment, the resistance across the surface of the electrodes was checked with a resistance meter and was always found to be negligible (<1 Ω). The effect of electrode hardening temperature on R_{add} for the LSGM ceramic measured using gold paste electrodes at 334°C is summarised in Fig. 7. The value of R_{add} peaked on hardening gold paste electrodes at 650°C overnight.

Z^* plots of a LSGM ceramic measured using platinum paste electrodes did not vary significantly with electrode hardening temperature up to and including 650°C. However, a small additional arc, with an associated resistance R_{add}, became distinct after heating at 725°C overnight. The additional arc diminished slightly relative to the bulk arc on subsequent heat treatments up to and including 1000°C. Estimated values of the capacitance associated with the additional arc were in the range ~10 to 40 nFcm^{-1}. The values of R_{add} for platinum paste electrodes as a function of electrode hardening temperature are also shown in Fig. 7. The resistance across the surface of the platinum paste electrodes was always found to be negligible (<1 Ω).

R_b measured using gold paste electrodes hardened at the different temperatures fluctuated around an average value of about 16 kΩcm at 334°C. R_b measured using platinum paste gave a similar value for hardening temperatures up to 850°C but increased by about 50% after hardening the electrodes at 1000°C.

When gold paste electrodes hardened at 650°C and exhibiting an additional arc in Z^* plots were removed by careful scraping with a scalpel, and new gold paste electrodes applied and dried at 200°C for 2 hours, the re-measured spectrum did not show the additional arc. This showed the component exhibiting the additional response was either within the gold paste electrode hardened at 650°C, or possibly directly on the surface of the ceramic, rather than within the interior of the ceramic. This eliminated the possibility that the low oxygen partial pressure during the burn out of the organics in the gold paste in air induced surface reduction of the LSGM ceramic.

Z^* plots of a LSGM ceramic with sputtered gold electrodes annealed at 650°C did not exhibit an additional impedance response. This showed that the large additional arc exhibited by ceramics with gold paste electrodes hardened at 650°C was not caused directly by a reaction with gold metal. The same result was obtained when a LSGM ceramic with sputtered gold electrodes was annealed at 650°C in a N_2 atmosphere, so eliminating the possibility of LSGM reacting with gold at low oxygen partial pressures, as might occur on a local scale during the burn out of organics in gold paste electrodes.

Micrographs of cross-sections of sputtered gold electrodes, and gold paste electrodes dried at 200°C for 2 hours and then hardened overnight at 350, 650 and 1000°C on LSGM ceramics are shown in Fig. 8. For all samples, the mounting resin split to varying extents along the electrode-ceramic interface during polishing, and it was assumed that this was not the original degree of electrode adherence during impedance measurements. All electrodes had negligible resistances across their surfaces. The resistance of sputtered gold electrodes was higher than the others but still negligibly small compared to the resistance of the ceramic. Of these samples, only the sample with gold paste electrodes hardened at 650°C exhibited a significant additional arc in Z^* plots. Sputtered gold electrodes consist of a layer less than 0.5 μm thick making an almost continuous contact with the pellet surface, Fig. 8(a). The gold paste electrodes hardened at 350°C consist of a ~12 μm thick layer of well-packed gold particles, which range from ~0.5 to 2 μm in size, Fig. 8(b). Although the gold particles have not sintered together,

the electrode appears to make good contact with the ceramic *via* numerous, discrete contacts. The morphology of the gold paste electrodes hardened at 650°C is significantly different. They consist of partially sintered gold particles, approximately 5 μm in diameter. These make isolated contacts ~1 μm in length approximately every 5 μm across the pellet surface, Fig. 8(c). The gold paste electrodes hardened at 1000°C consist of a ~6 μm thick uniform layer of gold formed by the complete sintering of the original gold particles. These electrodes make almost continuous contact with the ceramic surface, Fig. 8(d).

From the results presented, the major difference between the various ceramic-electrode samples tested appears to be the morphology of the electrode and the extent of contact with the ceramic surface. The

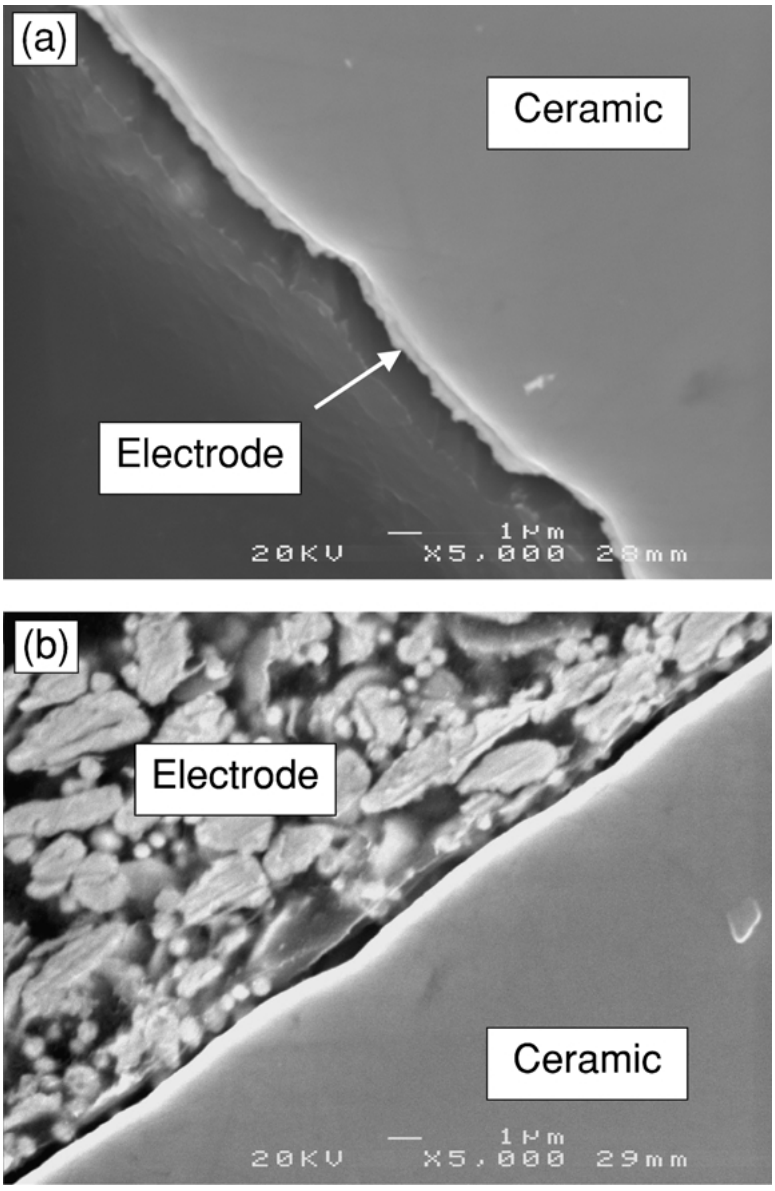

Fig. 8. SEM micrographs of cross-sections of sputtered gold electrodes (a), and gold paste electrodes dried at 200°C for 2 hours and then hardened overnight in air at 350°C (b), 650°C (c), and 1000°C (d) on LSGM ceramics.

(*Continued on next page*.)

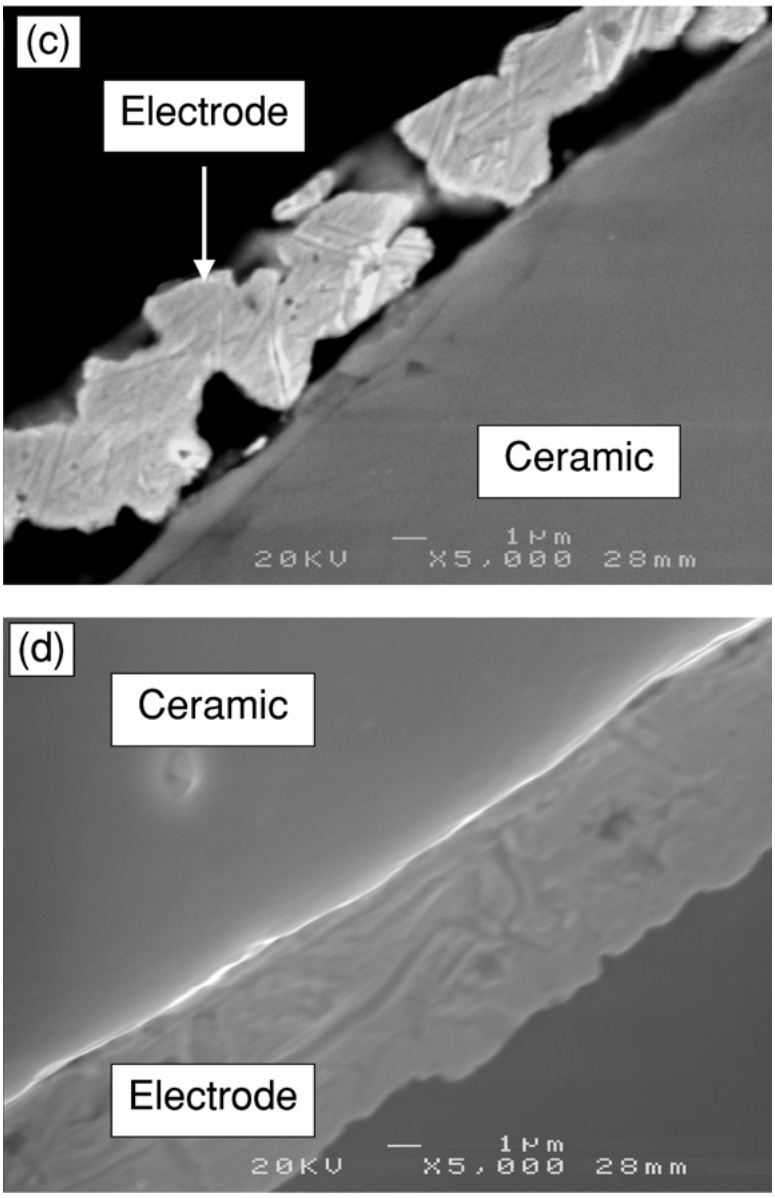

Fig. 8. (*Continued*).

electrode-sample configurations that gave rise to the additional, intermediate frequency impedance response with gold paste electrodes hardened between 500 and 850°C, correspond to those in which the electrode particles have partially sintered to form an electrode making discrete contacts with the LSGM ceramic surface. Various possible origins of the additional impedance have been considered and it is concluded that spreading resistances are responsible. The gradients of Arrhenius plots of the bulk resistance, R_b, and the resistance of the additional response, R_{add}, are very similar, Fig. 5, because the same oxide-ion conduction mechanism causes the bulk and additional responses. The presence of the air gap capacitance in the equivalent electrical circuit in Fig. 3 increases the time constant of the additional response compared to that of the bulk, hence they appear at different frequency ranges in Z^* plots. Gold paste electrodes hardened at 1000°C do

not exhibit the additional response associated with a spreading resistance since the gold particles have sintered completely to give an electrode making an almost continuous contact with the ceramic surface. Likewise, sputtered gold electrodes make a continuous contact with the ceramic surface and so do not exhibit a spreading resistance. The small additional response exhibited by platinum electrodes hardened at 725°C and above could also be due to spreading resistances caused in the same way. Spreading resistance does not occur if the discrete contacts are sufficiently close and numerous to avoid significant current constriction, as is the case for gold paste electrodes hardened at 350°C overnight. Under these conditions Eqs. (3) and (4) are invalid since the inter-contact distance is not significantly larger than the contact radii. Given the magnitude of capacitance associated with the spreading resistance response was $\sim$1 nFcm^{-1}, and the activation energy of its associated resistance was very similar to that of the bulk, its impedance response could have been mistakenly attributed to a grain boundary constriction resistance. This demonstrates the importance of using sputtered (gold) electrodes to distinguish between grain boundary and spreading resistance responses for samples coated with organo-paste electrodes.

The micrograph in Fig. 8(c) shows that for the LSGM ceramic with gold paste electrodes hardened at 650°C, about 30% of the electrode makes contact with the cross-section of the ceramic via well-separated discrete contacts. The inter-contact distance is about ten times larger than the radii of the contacts, so by assuming the contacts are approximately circular, the use of Eqs. (3) and (4) is justified. The total value of $\sum a$ calculated from the values of R_{spt} (where $R_{\text{spt}} = R_{\text{add}}$) and σ extracted from impedance spectra is approximately 1.4 mm. However, R_{add} represents the total spreading resistance of both electrodes, on either side of the ceramic, and assuming that both cause equal spreading resistance irrespective of their polarity, the total spreading resistance of each electrode is half of this value. Therefore the value of $\sum a$ for each electrode is 0.70 mm, and this is 14% of the radius of the ceramic. This is about half the value as estimated from the SEM micrograph. This discrepancy is probably due to errors in estimating the degree of ceramic-electrode contact. Since the distribution of contact radii is unknown it is not possible to convert the line fraction ($\sum a$/ceramic radius) into an area fraction. The value of the capacitance associated with the spreading resistance response is 1 nFcm^{-1}. This value is about 1000 times higher than

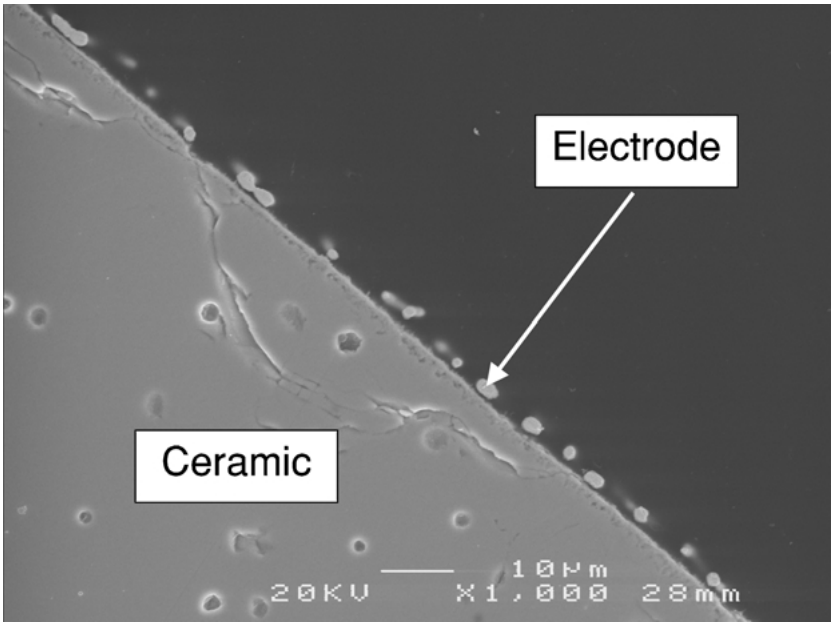

Fig. 9. SEM micrograph of the cross-section of platinum paste electrodes dried in air at 200°C for 2 hours and then subsequently hardened overnight at 1000°C on a LSGM ceramic.

that obtained by Hwang et al. [2]. The disparity could to be due to differences in size and shape of the air gaps generated when pressing gold foil directly onto a rough ceramic surface (Hwang et al.) as opposed to those contained in partially-sintered gold paste electrodes, as in the present study.

The experimental conditions to generate spreading resistances in an electroceramic with organo-paste electrodes are likely to depend on the hardening temperature and the ceramic material, but also on the composition of the paste. The viscosity of the paste, the metallic particle size distribution and the behaviour of any sintering aids present are all likely to influence the quality of the electrode. Whilst the importance of having electrodes which make approximately continuous contact with ceramic surfaces is clear, trying to achieve this by sintering organo-paste electrodes at high temperatures can cause other problems. It can lead to the loss of electrode coverage on pellet surfaces due to spallation, excessive sintering and partial melting of the electrodes. This can increase the 'apparent' measured value of the resistivity of the sample. Such a loss of electrode coverage was observed for platinum paste electrodes hardened at 1000°C. The resistance associated with the bulk response in Z^* plots for samples measured at 334°C using platinum paste electrodes increased by ∼50% when electrodes were hardened at 1000°C overnight. SEM of an electrode-ceramic interface for platinum electrodes hardened at 1000°C overnight showed large regions with little or no electrode, Fig. 9. This indicates that the increase in the 'apparent' resistivity of the ceramic is due to a loss of electrode area causing an increase in the effective geometric factor of the pellet. Spreading resistance was also observed on heating the platinum electrodes at 750°C and above and hence, two separate effects were seen with platinum, spreading resistance and loss of electrode coverage. For a spreading resistance effect, R_b is unchanged from the value obtained using sputtered gold electrodes, whereas for spallation R_b increases significantly.

Conclusions

Additional responses can be introduced into the impedance spectra of electroceramics such as doped-lanthanum gallate ceramics by using gold and platinum paste electrodes. The use of gold paste electrodes can lead to a significant additional response in Z^* plots, due to partial sintering of gold particles in paste electrodes hardened at temperatures ranging from 500 to 850°C. This produced an array of well-separated discrete electrode contacts with the ceramic, leading to the generation of spreading resistances due to oxide-ion current constriction. The spreading resistances had similar temperature dependence to the bulk resistance. The magnitude of the capacitance associated with the spreading resistance response was $\sim$1 nFcm^{-1} and could have been mistakenly attributed to a grain boundary constriction resistance response. Spreading resistances can be avoided by ensuring that electrodes make continuous contact across the sample surface by adequate sintering of conductive paste or by using sputtered electrodes. Impedance spectra measured using platinum paste electrodes hardened between 725 and 1000°C exhibited smaller spreading resistances but with similar behaviour to those detected using gold paste electrodes. Additionally, the overall contact area was significantly reduced for Pt electrodes fired at 1000°C, giving rise to an apparent increase in sample resistance.

Acknowledgments

We thank the EPSRC for a studentship (EJA).

References

1. J.T.S. Irvine, D.C. Sinclair, and A.R. West, *Adv. Mater.*, **2**, 132 (1990).
2. J. Hwang, K.S. Kirkpatrick, T.O. Mason, and E.J. Garboczi, *Solid State Ionics*, **98**, 93 (1997).
3. J.G. Fletcher, A.R. West, and J.T.S. Irvine, *J. Electrochem. Soc.*, **142**, 2650 (1995).
4. T. Kenjo and T. Nakagawa, *J. Electrochem. Soc.*, **143**, L92 (1996).
5. J. Newman, *J. Electrochem. Soc.*, **113**, 501 (1966).
6. R. Holm, *Electric Contacts: Theory and Application* (Springer-Verlag, New York, 1967).
7. E.J. Abram, D.C. Sinclair, and A.R. West, unpublished results.
8. K. Huang, R.S. Tichy, and J.B. Goodenough, *J. Am. Ceram. Soc.*, **81**, 2565 (1998).